

# Nonlinear Deterministic Methods for Computer Aided Diagnosis in Case of Kidney Diseases

Andreea Udrea, Mihai Tanase and Dumitru Popescu  
*Department of Automatics, University Politehnica of Bucharest, Bucharest, Romania*

**Keywords:** Computer Aided Diagnosis, Nonlinear Deterministic Methods, CT Images.

**Abstract:** This paper proposes a set of nonlinear deterministic methods derived from chaos theory that can serve as computed aided diagnosis tools for kidney diseases based on computer topographies (CT). These procedures target the classification of the analyzed tissue samples in normal, malign and benign affected and also enhanced visualization of the CT images. The classification methods consist in estimating the fractal dimension of the kidney tissue and, respectively, the correlation dimension of the attractor obtained from the spatial series associated to the kidney image. The enhanced visualization method associates a fractal map to the analysed image. The methods are tested on 120 CTs presenting normal and modified tissue. The degree of trustworthiness of the methods while dealing with classifications is discussed based on statistical results and samples of fractal maps associated to the images are also presented.

## 1 INTRODUCTION

In order to increase the life expectancy and improve the overall quality of life for patients with kidney diseases, a critical stage in the medical process is to employ a suitable protocol for delivering the diagnostic, establish a treatment and, when needed, to design an appropriate follow up procedure. Usually, the first investigations and the follow up consist in noninvasive or minimally invasive procedures, in order to obtain the biological data for proposing an accurate diagnostic. In this context, any improvement in interpreting the patient's data is highly important.

When considering such data, at least two main problems of tremendous importance have to be solved: capturing and storing the considered medical signals, on one hand and, on the other hand, analyzing and interpreting the stored signal. In order to capture 2D signals of the kidneys the most used procedure is computer tomography (CT). The obtained signals (grey level images) are usually highly nonlinear, rather noisy and due to close values of radio densities of the tissues, sometimes difficult to interpret.

Analysis and interpretation of the captured medical signals is almost exclusively subjected to the human diagnosis expertise and experience. In the last decade, a lot of effort was made to create

automatic analysis and diagnosis tools for aiding the medical act. Nowadays, automatic diagnostic is still a long term goal to be achieved, but Computer-Aided Diagnosis (CAD) systems design seems possible. This is confirmed by all major medical imaging companies increasing interest in developing CAD systems. Three signal processing operations are closely related to CAD topics: filtering, segmentation and quantification of analyzed features. Enhanced visualization is another important aspect, especially in the context of kidney CT images presenting benign affected tissue.

The main goal of this paper is to present a series of new or improved nonlinear methods that can aid the medical diagnostic in the case of kidney diseases and can be included in a CAD system. These methods are derived from nonlinear time series analysis and fractal geometry, both branches of chaos theory. Their primary goal is to analyze the kidney CT images and to decide if the presented tissue is normal, malign affected, benign affected and also to try differentiating between types of benign diseases and malignancy stages. Where these classification attempts prove limitations, enhanced visualization procedures are offered as support.

The paper is organized in four chapters. In what follows the nonlinear deterministic methods to be used are presented and the results obtained by employing them to the analysis of CTs are

statistically analyzed. For this study, a series of 120 CT images were used: fifty of them contain malign modified kidney tissue, fifty images present normal kidney tissue and the rest of twenty are organised in four images groups of benign affections. In the end conclusions are summarized.

## 2 THE PROPOSED NONLINEAR DETERMINISTIC METHODS FOR CAD

Nonlinear time series analysis (NTSA) and fractal analysis, as branches of chaos theory, provide useful methods for the characterization of mono and multi variable signals (like time series and images).

### 2.1 Attractor's Correlation Dimension Estimation Method for the CT Image Associated Time Series

Typically, the NTSA deals with series that are sets of values of a single variable function, usually measured as function of time (dynamic features). Nonlinear methods have been developed in the past 20 years, being motivated by the concept of deterministic chaos, which is proved to exist within many real systems in biology, medicine, chemistry, physics and electronics. The studied time series in medicine and biology are: recordings of the electrical activity – electrocardiograms (EKG), electroencephalograms (EEG) and physiological parameters – blood pressure, pulse, and breathing rate. Here are some applications with important results of NTSA: diagnosis and control of cardiac arrhythmia and ventricular fibrillations prediction (Perc, 2005); characterization of sleep stages (Rajendra, 2005); evaluation of variations in brain functioning for psychical processes characterization (Mekler, 2008; Pritchard and Duke 1995); characterization of anesthesia state (Widman, 2000).

The proposed NTSA derived method is based on the invariant measure of a chaotic dynamical system: the correlation dimension of the system's attractor. By investigating time series, one can observe the behavior and properties of dynamical systems, in our case of different physiological parameters.

From the mathematical point of view, there is a formalism to describe the time series features. Let the real valued map  $F : M \rightarrow \mathbf{R}$  be a measure on the state space of some discrete dynamical system  $T$  providing data in  $M$ . If  $s > 0$  is a fixed delay (assigned to some sampling period) and  $x$  is a fixed

state, then a time series is a sequence of measurements like the following:

$$F(T(t,x)), F(T(t+s,x)), F(T(t+2s,x)), \dots, F(T(t+(N-1)s,x)) \quad (1)$$

for any starting instant  $t$ . Note that the state changes too during the time series acquisition. The samples of time series are often simply denoted by  $x_t, x_{t+1}, x_{t+2}, \dots$ . In context of medical signals, these time series are measurement (like EEG, EKG) performed on some patient (represented here by the system  $T$ ). The acquisition rate and the length of the measurement depend on the type of investigated parameter. One can reconstruct the attractor of a dynamical system from the time series generated by the system, by using the Taken's Embedding Theorem (Taken, 1981) and computing the correlation dimension of the attractor in order to geometrically characterize it. The correlation dimension  $d_C$  is calculated using the following recipe:

$$C(\varepsilon) = \varepsilon^{d_C}, \varepsilon \rightarrow 0 \Rightarrow d_C = \lim_{\varepsilon \rightarrow 0} \frac{\ln C(\varepsilon)}{\ln \varepsilon} \quad (2)$$

where  $C(\varepsilon)$  is the correlation integral defined below:

$$C(\varepsilon) = \lim_{N \rightarrow \infty} \frac{1}{N^2} \sum_{i,j=1}^N H(\varepsilon - |y_i - y_j|) \quad (3)$$

and:  $H$  is the Heaviside step function (which returns either the unit value for non negative arguments or null value otherwise),  $\varepsilon$  is the accepted distance between points,  $y_i$  is a point in the embedded phase space constructed from a single time series, according to Taken's theorem, i.e:  $y_i = (x_i, x_{i+s}, x_{i+2s}, \dots, x_{i+(d_E-1)s})$ ,  $s$  is the delay,  $d_E$  is the dimension of the embedding space where the attractor resides,  $N$  is the number of embedding vectors. So,  $C(\varepsilon)$  gives the proportion of number of points couples in the embedding space with the Euclidian distance less than a specified small threshold  $\varepsilon$ .

In pathology (especially in case of CT, RM images and frozen tissues samples), one deals with static (invariant) structures. In this case, measurements are taken with respect to the one-dimensional spatial axis, instead of temporal axis. In this context we propose a method for reconstructing the attractor from a CT image an associate to it a specific  $d_C$ .

In order to perform nonlinear analysis on a CT normal or modified tissue image, a series of steps must be made.

First, from a CT slice, the region containing the tissue to be analyzed must be isolated; a matrix containing values of each pixels shade is obtained (the value can vary between 0 and 255 corresponding to different shades of grey; 0 stands for black and 255 for white). The time (spatial) series is generated in the following manner: the matrix resulting from the original image is cut in horizontal strips of 1, 2, 4, 8, ... pixels, with respect to the initial image dimension and precision; all strips are put together one after another and generate one single strip associated to the image; the time (spatial) series -  $x(t)$  - is generated by computing either the mean value or the maximal (dominant) value of each column of pixels within the strip.

As result of this procedure, the time (spatial) series associated to the section of the analyzed tissue is obtained. For this study, since the analyzed CT regions are not extremely large, a 1-pixel strip was associated to each original image, this way not altering the information provided by the image.

Having the associated series, the next step of the procedure implies calculating the correlation dimension of the attractor. This value is the discrimination criterion.

However, in practical applications, in order to determine the dimension of an attractor, we cannot directly use the above formulae for  $d_C$  due to the following aspects: limited time series; noisy time series; unknown fractal dimension of the attractor; for different  $s$  - delay values different results due autocorrelations; unknown  $d_E$  - leading to time correlations when reconstructing the series in a embedding space with unsuitable dimension; time series with the first part of data not on the attractor.

The delay or lag value  $s$  used to create the delayed embedding must be properly chosen (Kantz and Schreiber, 2003). A small value of the delay generates correlated vector elements, while large delay values yield to uncorrelated data and a random distribution in the embedding space. The delay can be chosen with good results as the moment of time where the autocorrelation function of the reconstructed series decays to  $1/e$  of its initial value:

$$RN(\tau) < RN(1)(1 - 1/e). \quad (4)$$

Generally, the lag value is found between 4 and 10, while the used search interval is [1, 20].

The minimum allowed embedding dimension is the dimension where the number of so called false nearest neighbours drops under a certain percent. A false neighbour is a point that under a certain higher dimensional embedding is projected near a point that in the previous embedding is not in its vicinity.

In order to implement this procedure, each point of the delayed series is tested by taking its closest neighbour in  $d_E$  dimensions, and computing the ratio of the distances between these two points in  $d_E + 1$  dimensions and in  $d_E$  dimensions. If this ratio is larger than a certain threshold  $th$ , the neighbour is false (this threshold is taken large enough to take in consideration points that exponential diverge due to deterministic chaos):

$$\frac{\|y_{i,d_{E+1}} - y_{j,d_{E+1}}\|}{\|y_{i,d_E} - y_{j,d_E}\|} > th \quad (5)$$

where  $\|\cdot\|$  is the Euclidian distance.

The percentage of false neighbours is computed over a range of embedding dimensions ( $d_E$  between 2 and 15) until it reaches a value less than a specified limit; otherwise it considers the minimal obtained value.

Once a proper delay and a minimum allowed embedding dimension are determined, the correlation dimension is calculated over a range of different  $\epsilon$  - values and embedding dimensions higher than the first assuring a decreased number of false neighbours.

The  $d_C$  differs from one embedding dimension to another due to the noise in the data, but there is a particular region, usually called the *scaling region* where  $d_C$  stabilizes (Kantz and Schreiber, 2003). This is the interval where a mean value for the correlation dimension of an attractor is calculated.

## 2.2 The Box-Counting Dimension Estimation Method

Fractal analysis methods are used for the description and quantization of geometric features of irregular forms and patterns. Its most known tool is the fractal dimension used to provide information on the irregularity of an object contour or self-similarities of a texture, which associates to some pathology as well. It was applied for the study of medical systems and subsystems at microscopic and macroscopic scale, fracture analysis or texture classification (Peitgen, 1992). The simplest medical application consists in the morphological analysis of a structure (for example, the lung network of arteries and veins). This analysis of irregularities can be applied in a similar manner on different forms, like the delimitation between normal and affected tissue, lesions, and tumors.

Here are some examples of fractal analysis results in medicine and biology: classification in pathology (Bassingthwaighte, 1994; Dobrescu si

Vasilescu, 2004) and physiology (Luzi, 1999), tumor growth description (Landini, 1998). The box counting method provides a measure of fractal dimension  $d_f$  estimated for texture or contour.

The  $d_f$ , derived from the Hausdorff coverage dimension, is given by the following approximation:

$$d_f = \lim_{s \rightarrow 0} \frac{\log(N(s))}{\log(1/s)} \quad (6)$$

where: -  $N(s)$  is the number of squares with side length  $s$  that contain information when grid covering the image.

Relation (6) is the equation of the slope  $d_f$  of the regression line associated to the points  $(\log(N(s)), \log(1/s))$  for different values of the square's side -  $s$  of the covering grid..

The standard Box-Counting algorithm assumes to determine the  $d_f$  in accordance with the dependence of the texture upon the used scale factor. It consists transforming the grey scale image in binary image, successively covering it with a grid of squares of equal sides  $(2, 2^2, 2^3, \dots)$  and counting each time the squares that contain some part of the analyzed object. The points of coordinates  $(\log(N(s)), \log(1/s))$  are approximately positioned in a line and its slope is the fractal dimension in "box-counting" sense.

To exemplify how the algorithm is used, we'll consider the image of a kidney (Figure 1. a)) from which we'll extract a binary version by neglecting all the pixels over a certain threshold (Figure 1. b)).

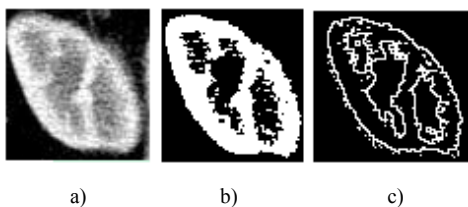


Figure 1: a) The original image; b) binary image c) extracted contour.

Next, we'll apply the box-counting algorithm, described above, for different scale values  $s$ .

This method can be also used to determine the self similarities of an object contour (Figure 1 c)), but in our case, due to the fact that the kidney capsule is not necessary affected, the texture is more important.

A general problem of this method is the use of an ad hoc threshold when creating the binary image. This fact leads to incomplete or "noisy" object in the binary image and sometimes importantly affects the fractal dimension value.

### 2.3 Weighted Box-Counting Dimension for Image Enhancement

This algorithm is based on the fact that in the CT images a higher density of the tissue is equivalent to lighter gray. Our idea was to associate to every pixel a weight proportional to its gray level. We resume the essential of the algorithm below.

Let us consider an image. We cover the image with square boxes as in the standard Box-Counting algorithm. Let  $s_k$  be the size of the box used in covering at step  $k$  (therefore we have to compute  $N(s_k)$  at this step). Let  $(x, y)$  be the coordinate of the upper-left corner of one of these boxes (let this be the box  $B_t^k$ ).

We now define  $m_t^k$  as the maximum of the weight values of the pixels contained in this box.

$$m_t^k = \max\{w_{i,j} \mid (i,j) \in ([x, y] \times [x + s_k - 1, y + s_k - 1]) \cap Z \times Z\} \quad (7)$$

where  $w_{i,j}$  is the weight associated to the pixel at  $(i,j)$  coordinates.

Let  $W_t^k = [m_t^k / s_k] + r_t^k$ , where if  $s_k \mid m_t^k$  then  $r_t^k = 1$  else  $r_t^k = 0$ .

$$\text{Therefore } N(s_k) = \sum_t W_t^k.$$

Next, the computation formula for  $d_w$  is the similar to the one in the classical algorithm. We shall refer to the number  $d_w$  as the Weighted Box Counting Dimension or WBCD. Let us consider an image and let  $A$  be a pixel on it. Let  $K$  be a square centered at  $A$ . By using the previous algorithm we compute the WBCD of the square  $K$  and we associate a color to the pixel  $A$  according to this WBCD (the function which associates the color is a key part of the algorithm). This way we obtain a map of level lines (we shall refer to this map as the Fractal Map or FM).

This leads to a classification of different tissues according to the associated color. Different structures must have different colors. The use of the FM in diagnosis requires a database with sufficient images.

## 3 RESULTS AND STATISTICS

We start the analysis procedure by presenting the statistical results obtained by using  $d_f$  and  $d_c$  as

classification methods. One hundred and twenty CT images were analysed; they were divided into two equal samples: containing normal tissue and half modified tissue.

For the statistical analysis, descriptive and comparison procedures were performed. For each sample, the average, standard deviation, standard skewness and standard kurtosis were computed.

In order to compare the samples the t test and Kolmogorov-Smirnov test were performed.

In the case of  $d_f$  both comparison tests show no significant difference between the two distributions at the 95.0% confidence level. So, the trustworthiness of this classification is low.

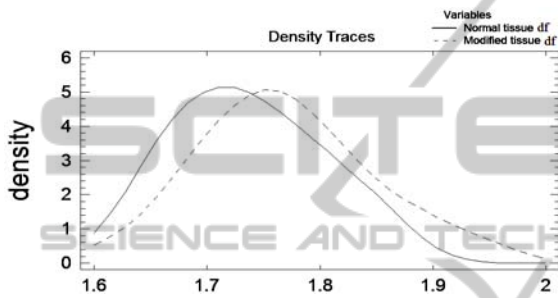


Figure 2: Comparison of density traces.

In the case of  $d_c$  both comparison tests show significant difference between the two distributions at the 95.0% confidence level.

The average is 1.729 for the normal tissue and respectively 1.974 for the modified tissue.

The 95.0% confidence interval for mean is [1.6282,1.83155] for the normal tissue and [1.87225,2.07725] for the modified tissue.

We conclude that the box-counting method is using a certain threshold, this way losing some information on the tissue texture while nonlinear analysis is more precise and uses all the information in the images. We recommend the use of the second method for analyzing CT images.

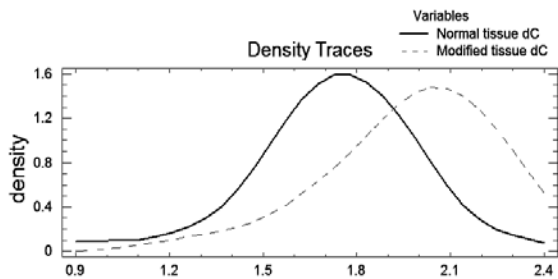


Figure 3: Comparison of density traces.

We have also compared the results acquired when the CT was taken with contrast substances and

without. In the second case, the  $d_c$  values are smaller because of a series of features that are not so visible (blood vessels). The differences between the  $d_c$  of normal and modified tissue samples are smaller. So, we suggest that this methodology is better to be used with associated time series resulting from CT images taken with contrast substances.

The second step in the analysis was to determine the correlation dimension of the attractor for images containing kidneys with benign affections.

The discrimination is obvious in the cases of pyelonephritis (the resulted  $d_c$  values being smaller than in the case of normal tissue) and kidney tuberculosis (with  $d_c$  values larger than in the case of malign modified tissue).

Table 1: Benign modified tissue images, their fractal maps and associated  $d_c$  values.

Affection	Image	Enhanced	$d_c$
Pyelonephritis			1.36 (correspondent $d_c$ for healthy kidney -1.85)
Medullary sponge kidney			1.91(1.86)
Polycystic kidney			2.06 (1.9)
Kidney tuberculosis (renal TB)			2.3(1.92)
Thrombosis			1.98(1.93)

The  $d_c$  values for medullary sponge kidney tissue and thrombosis affected kidney tissue are generally a little bit larger than the ones for normal tissue.

The  $d_C$  values for polycystic kidney tissue were generally larger than the ones for normal tissue.

In the third column of the above table the kidney CT image fractal map is presented.

The kidney border and affection specific aspects like different types of tissue clusters and their delimitation can be seen clearer.

Also, the different colours in the map identify different formations, specific to the affection.

This method proved more useful than the previous two in aiding the diagnostic in the case of benign affected tissue.

We conclude that discrimination between these benign affections can be done but needs a larger database of images.

Further work will focus on enlarging the CT images data base in order to provide more accurate discrimination interval values for different types of kidney affections.

#### 4 CONCLUSIONS

The conclusions of the study on the selected set of CT images are: there are significant differences between the correlation dimension of the normal tissue and the correlation dimension of the modified tissue; significantly better results are obtained in the case of CT images taken when contrast substances are used. The proposed nonlinear method for estimated the correlation dimension associated to a CT image proved efficient for differentiating between normal and modified kidney tissue while the box-counting method failed in providing useful results. The image enhancement method proved very helpful when inconclusive classification was obtained for benign tissue.

Future work aims at: enlarging the CT images data base; creating the fractal model of the kidney, measuring, where it is possible, the percentage of the modified tissue in a kidney CT slice in order to provide information on what is causing the increase in  $d_C$  (percentage of affected tissue or  $d_C$  value of modified tissue); determining the position of masses in an affected organ when considering horizontal slices and respectively reconstructed transversal slices in that organ .

#### REFERENCES

Bassingthwaight J. B., Liebovitch L. S., West B. J., 1994. *Fractal Physiology*. Oxford University Press

Dobrescu R., Vasilescu C., 2004. Interdisciplinary applications of fractal and chaos theory. *Romanian Academy Press*, pp. 247-254, 2004

Luzi P., Bianciardi G., Miracco C., De Santi M.M., Del Vecchio M., Alia L., Tosi P., 1999. Fractal analysis in human pathology. *Ann. N.Y. Acad. Sci.* 879, 255-257

Landini G., 1998. Complexity in tumor growth patterns, *Fractals in Biology and Medicine*. Birkhäuser Verlag, pp. 268-284

Kantz H., Schreiber T., 2003. *Nonlinear time series analysis*, 2003. Cambridge University Press, 3<sup>rd</sup> edition

Mekler A., 2008. Calculation of EEG correlation dimension: Large massifs of experimental data. *Computer Methods and Programs in Biomedicine*, vol. 92, pp. 154-160

Peitgen H. O., Jurgens H., Saupe D., 1992. Chaos and Fractals – New Frontiers of Science. Springer-Verlag

Perc M., 2005. Nonlinear time series analysis of human electrocardiogram. In *European Journal of Physics*, vol. 26, pp. 757-768.

Pritchard W. S., Duke D. W., 1995. Measuring chaos in the brain: A tutorial review of EEG dimension estimation. *Brain Cognition*, vol. 27, pp. 353-397

Rajendra U., Faust O., Kannathal N., Chua T., Laxminarayan S., 2005. Non-linear Analysis of EEG Signals at Various sleep stages. In *Computer Methods and Programs in Biomedicine*, vol. 80, pp. 37-45.

Takens F., 1981. Detecting strange attractors in fluid turbulence. In *Dynamical System and Turbulence*, Rand D. A., Young, L. S. (Eds), *Lecture Notes in Mathematics*, Springer Verlag

Widman G., Schreiber T., Rehberg B., Hoerof A., Elger C. E., 2000. Quantification of depth of anesthesia by nonlinear time series analysis of brain electrical activity. *Physical Review E*, no. 62, pp. 4898-4903